Current-phase relation in a short clean josephson junction model: application to MgB_2

Journal of Physics Communications

OPEN ACCESS

RECEIVED
10 September 2019

ACCEPTED FOR PUBLICATION
21 February 2020

PUBLISHED
18 March 2020

PAPER

Current-phase relation in a short clean josephson junction model: application to MgB_2

Y D Agassi[1] and Daniel E Oates[2]

[1] Consultant, Jerusalem, Israel
[2] MIT-Lincoln Laboratory, 244 Wood St., Lexington, MA 02421-6426, United States of America

E-mail: oates@ll.mit.edu

Keywords: josephson junctions, green's function, superconductivity, energy-gap symmetry, magnesium diboride

Abstract

Motivated by recent data on high-quality MgB_2 thin films implying that the smaller energy gap has $l = 6$ (i-wave) symmetry, we consider a simple model for an all-MgB_2 symmetric Josephson Junction (JJ). The model assumes an arbitrary-strength delta-function barrier and one-dimensional current conduction. It is shown that in this context a nodal energy gap with i-wave symmetry acts as an isotropic energy gap (s-wave) with an amplitude modified by the energy-gap misalignment-angle with respect to the crystal principal axes. The corresponding exact Green's function in momentum space is derived employing a novel approach. The ensuing current-phase relations in the strong and weak barrier-strengths limits are calculated and found to confirm known results, e.g., the Ambegaokar-Baratoff current-phase relation. Inspired by an HTS experiment that established the d-wave energy-gap symmetry, we propose a JJ-related experiment with a MgB_2 bicrystal to confirm our premise that the smaller energy has i-wave symmetry.

1. Introduction

An important aspect of the MgB_2 superconductor is its potential technological advantages over the cuprate high-temperature superconductors (HTS). Specifically, its relatively high critical temperature ($T_C \approx 40$ K) simplifies cryogenic requirements, its relatively long coherence length avoids the problem of grain boundaries acting as weak links, and its stoichiometry and crystal structure are simple [1–5]. These advantages continue to stimulate substantial work on power applications such as conductors, RF cavities, and digital applications to mention a few [6–11].

From a physics point of view MgB_2 is interesting in at least two respects. It has two energy gaps that are susceptible only to weak coupling by non-magnetic impurities and, allegedly, these two energy gaps have distinct symmetries [12–15]. By convention, the two energy gaps are labelled as the σ (larger) and the π gap (smaller). Whereas the symmetry of the σ energy gap is s-wave [1, 3], recent low-temperature microwave-frequency measurements of the intermodulation distortion (IMD) strongly suggest for the π energy gap an i-wave ($l = 6$) symmetry [13]. The IMD low-temperature variation provides a signature for a nodal energy gap [16, 17]. This signature been observed in the cuprate YBCO which indeed has a nodal (d-wave) energy-gap. The measured low-temperature IMD of MgB_2 is strikingly similar to that of YBCO, which strongly suggests a nodal π energy gap, specifically with i-wave symmetry [15]. Other observables, such as the low-temperature penetration-depth anomaly and the temperature dependence of the microwave surface resistance provide additional support for the i-wave symmetry [13]. With its two energy gaps having different symmetries MgB_2 is so far unique.

Theoretical calculations predict and tunneling experiments confirm that the π energy gap plays a prominent role in current conduction [11, 18, 19]. Specifically, current conduction in both the $\hat{c}$ direction and in directions close but not equal to the *ab* plane is expected to be dominated by the π energy gap. This is consistent with the three-dimensional Fermi surface that underlies the π energy gap, in contrast to the approximately two-dimensional Fermi surface underlying the σ energy gap [1, 20, 21]. Given the π-gap role in current conduction and the evidence of its nodal symmetry, we consider here the impact of the i-wave symmetry on the current-

phase relation (CPR) in all-MgB_2 Josephson junctions (JJ) [22–24]. To the best of our knowledge such an analysis does not exist. In view of the recent demonstration of $MgB_2/MgO/MgB_2$ junctions with a high critical current, the CPR calculation of an all-MgB_2 junction seems timely [11].

The CPR is calculated in a model that assumes a delta-function barrier and one-dimensional conduction in the direction normal to the barrier's plane. One-dimensional current conduction and this type of barrier have been employed before in the context of the Blonder-Tinkham-Klapwijk (BTK) analysis of SN tunneling with conventional superconductors, and for simulating multiple Andreev reflections in the barrier domain [25–27]. In this sense, our work represents an extension of this research.

As shown in section 2, a key approximation underlying this work is the reduction of a nodal energy gap to a constant (isotropic) energy gap with a properly modified amplitude. In particular, for an i-wave-symmetry energy gap this reduction takes the form

$$\Delta_i(\vec{K}) = \Delta_0 \ \sin(6(\varphi + \alpha)) \Rightarrow \Delta_0 \sin(6\alpha) \equiv \Delta_0(\alpha), \ \frac{2\pi}{6} \geqslant \alpha \geqslant 0, \tag{1.1}$$

where $\Delta_i(\vec{K})$ is the i-wave energy gap, $\vec{K}$ denotes the relative pair-momentum in the *ab* plane, φ is the azimuthal angle, Δ_0 is the energy-gap amplitude, and α is the barrier misalignment angle with respect to the crystal axes in the *xy* plane. When applied to a d-wave energy gap, the same reduction procedure yields

$$\Delta_d(\vec{K}) = \Delta_0 \cos(2(\varphi + \alpha)) \Rightarrow \Delta_0 \cos(2\,\alpha), \quad \frac{2\pi}{2} \geqslant \alpha \geqslant 0. \tag{1.2}$$

In the HTS context, the reduction (1.2) yields a CPR of structure consistent to that based on group-theoretic considerations; see appendix A [28, 29]. The energy-gap reductions, equations (1.1), (1.2), simplifies the analysis substantially.

In the literature there are several approaches to the calculation of the CPR for s-wave superconductors, e.g., the Bogoliubov–de Gennes equations, the Green's function approach and the Boltzmann equation [30–33]. The choice of approach is a matter of mathematical convenience for the objective at hand. In this work, we adopt the Green's function approach, originally devised to treat spatially varying perturbations in superconductors, such as a non-constant energy gap and impurities [34–36]. The JJ configuration fits into this category since the energy gaps on both sides of the barrier are different. There has been work to construct a real-space JJ Green's function [37, 38]. It is shown here that working in momentum space yields the *exact* Green's function for an *arbitrary* barrier strength. The ensuing CPR in the weak and strong barrier-strength limits is consistent with known results, e.g., Ambegoakar-Baratoff [33]. We emphasize that while the Ambegoakar-Baratoff CPR is applicable in the limit where the coupling between the two banks is weak (or a strong barrier-strength), the present Green's-function approach yields, in principle, the CPR for an arbitrary barrier strengths. The premise of one-dimensional current conduction normal to the barrier's plane, common to a wide body of works, is further discussed in the concluding section [39].

This paper is organized as follows. In section 2 the nodal energy-gap reduction, equation (1.1) is derived. Section 3 is devoted to the derivation of the exact Green's function in momentum space, and evaluating the ensuing CPR in the weak and strong barrier-strength limits. In section 4 we outline a generalization of the Green's function approach to accounts for weak coupling between the two energy gaps, e.g., by doping , suggestions for JJ-based experiments to confirm the i-wave π energy-gap symmetry, and a summary.

2. Nodal energy-gap reduction

In momentum space and cylindrical coordinates the nodal i-wave energy gap, $\Delta_i(\vec{K})$ is given by equation (1.1). Denoting by $\vec{x} = (\vec{\rho}, \ z)$, the corresponding real-space functional form is

$$\Delta_i(\vec{x} - \vec{x}'; \alpha) = \delta(z - z')\frac{\Delta_0}{(2\,\pi)^2}\int_0^{2\pi} d\varphi \int_0^{\infty} dQ\, Q\, e^{\,i\,\vec{Q}\cdot(\vec{\rho}\,-\,\vec{\rho}')} \sin(6(\varphi + \alpha)). \tag{2.1}$$

Noting that $\vec{Q} = Q(\cos(\varphi), \ \sin(\varphi))$, and denoting by γ the azimuthal angle of the vector $\vec{\rho} - \vec{\rho}' = |\Delta\vec{\rho}|(\cos(\gamma), \ \sin(\gamma))$, it follows that $\vec{Q}\cdot(\vec{\rho} - \vec{\rho}') = Q|\Delta\vec{\rho}|\cos(\varphi - \gamma)$. Employing the expansion [40]

$$e^{i\,z\,\cos(\gamma)} = \sum_{m=-\infty}^{\infty} i^m J_m(z) e^{i\,m\,\gamma}, \tag{2.2}$$

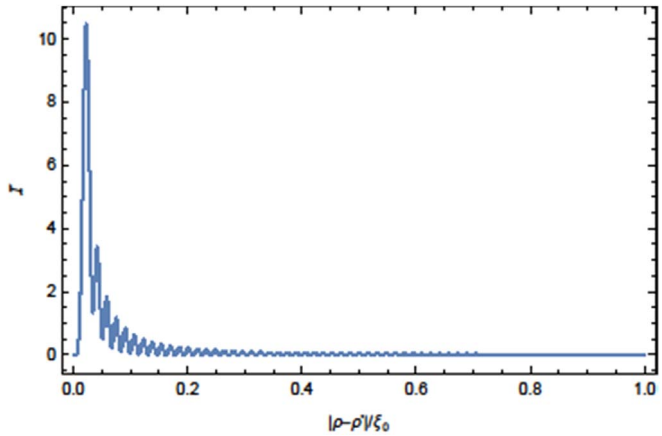

Figure 1. The calculated dimensionless integral in equation (2.3), for the following parameters: $k_F\ \xi_0 = 40$ and upper integration-limit cutoff at $\tilde{Q} = 10$. Increasing the cutoff sharpens and increase the peak near (however, never at) $\tilde{Q} = 0$.

where $J_m(z)$ denotes the Bessel function of order m, straightforward manipulation yields

$$\Delta_i(\vec{x} - \vec{x}';\ \alpha) = \delta(z - z')\left(-\frac{\Delta_0}{2\pi}\right)\sin(6(\gamma + \alpha))k_F{}^2 \int_0^\infty d\tilde{Q}\ \tilde{Q}\ J_6((k_F\ \xi_0)\ \tilde{Q}|\tilde{\vec{\rho}} - \tilde{\vec{\rho}}'|)$$
$$\tilde{Q} = Q/k_F, \quad \tilde{\vec{\rho}} - \tilde{\vec{\rho}}' = (\vec{\rho} - \vec{\rho}')/\xi_0.$$

In (2.3) ξ_0 and k_F denote the $T = 0$ K coherence length and the Fermi momentum, respectively.

Consider first the azimuthal angle γ. The vector $\vec{\rho} - \vec{\rho}'$ may point in any direction in the xy plane. However, under the assumption of one-dimensional current flow normal to the barrier's plane (at $x = 0$) it follows that only vectors $\vec{\rho} - \vec{\rho}'$ with $\gamma \approx 0,\ \pi$ need be considered. Consequently, in (2.3) we can write $\sin(6(\gamma + \alpha)) \approx \sin(6\ \alpha)$. Next consider the divergent dimensionless integral in equation (2.3), plotted in figure 1 for values pertinent to MgB_2, i.e., $k_F\ \xi_0 = 40$ and a chosen large cutoff [3]. As figure 1 shows, this integral diverges near the origin, however *not* at the origin. This real space divergence resembles the divergence of s-wave energy-gap in real space, as embodied by a delta function [34]. Here, however, and as expected for a nodal energy gap in real space, it has a finite range on atomic scale [36]. In the present context of a *global* property, i.e., the CPR, we adopt the approximation of ignoring the finite-range aspect of the nodal energy gap. Specifically, the divergent integral in equation (2.3) is approximated as

$$\frac{k_F^2}{2\pi}\int_0^\infty d\tilde{Q}\tilde{Q}J_6((k_F\xi_0)\tilde{Q}|(\tilde{\vec{\rho}} - \tilde{\vec{\rho}}')|) \approx \delta(\vec{\rho} - \vec{\rho}') \tag{2.4}$$

where the $k_F{}^2$ factor in (2.4) has been added to keep the correct dimensionality of the integral (ℓ^{-2} where ℓ denotes the length dimension).

The *overall* minus sign in equation (2.3) is of no consequence since, as shown in section 3 and appendix A only products of two energy gaps enter the CPR expression. Consequently the minus sign in equation (2.3) is henceforth ignored. All these considerations yield for the i-wave ($l = 6$) energy gap, equation (2.3), the reduced form

$$\Delta_i(\vec{x} - \vec{x}';\ \alpha) \approx \delta(z - z')\delta(\vec{\rho} - \vec{\rho}')\sin(6\ \alpha)\Delta_0 = \delta(\vec{x} - \vec{x}')\ \Delta_0(\alpha). \tag{2.5}$$

Equation (2.5) implies that in the present context, a nodal i-wave energy gap acts as a isotropic (s-wave) energy gap, however, with an amplitude modified according to the misalignment angle α. When applying the same line of arguments for a d-wave energy gap, as in YBCO, we obtain equation (1.2). As shown in next section and appendix A, the CPR is proportional to the product of the two energy-gaps on both JJ banks. Hence equation (1.2) leads to a CPR expression identical to that obtained from group-theoretic considerations [29].

3. The exact JJ Green's function

Following energy-gap reduction, equation (2.5), we consider a simplified symmetric s-wave JJ model with the objective of calculating the CPR. This model corresponds to a SIS all-MgB_2 Josephson junction. The barrier in this model is treated as a delta function of arbitrary strength in the absence of a voltage and a magnetic field. This particular barrier has been successfully employed in the BTK model for SN tunneling and related studies

[25, 26]. To the best of our knowledge, our approach to the CPR calculation differs from the large body of literature on s-wave JJ [33, 39]. Specifically, starting from the *integral form* of the Gorkov equation we solve for the exact JJ Green's function for an arbitrary barrier strength. Subsequently we derive the ensuing CPR in the common limits of strong and weak barrier strength [35]. A bonus of the present calculation is an explicit expression for the JJ critical current in terms of the barrier's strength. In this section we outline the approach and quote results. Details are deferred to appendix A.

In the one-dimensional coordinate space along the x axis the integral form of the Gorkov equation for the Green's function $G(x,\ x';\ \ \omega_n)$ and current-density expression $j(x)$ are

$$\begin{aligned} G(x,\ x';\ \omega_n) &= G_0(x,\ x';\ \omega_n) - \int_{-\infty}^{\infty} d\ x_1\ K(x,\ \ x_1;\ \omega_n)\ \ G(x_1,\ x';\ \omega_n), \\ K(x,\ x_1;\ \omega_n) &= \left(\tfrac{1}{\hbar^2}\right)\int_{-\infty}^{\infty} d\ x_1' G_0(x,\ x_1';\ \omega_n)\Delta(x_1') \times\ G_{\ 0}(x_1,\ x_1';\ -\omega_n)\Delta^*(x_1). \\ j(x) &= \left(\tfrac{1}{\beta\ \hbar}\right)\left(\tfrac{i\ \hbar\ q_S}{m}\right)\sum_{n=-\infty}^{\infty}(\nabla_{x'} - \nabla_x)G(x,\ x';\ \omega_n)|_{x'->x+}. \\ \omega_n &= \tfrac{(2\ n+1)\pi}{\beta\ \hbar}, \quad \text{for all n values.} \end{aligned} \tag{3.1}$$

In (3.1) $G_0(x,\ x';\ \omega_n)$ is the unperturbed Green's function that pertains to all interactions except pairing. In particular it includes the barrier. The symbol $\Delta(x)$ denotes the spatially dependent energy gap, q_S is the single-carrier charge (positive or negative), $\beta = 1/(k_B T)$ where k_B, T denote the Boltzmann constant and temperature, respectively, $\hbar$ is the normalized Planck's constant, and ω_n denotes the Matsubara frequencies [41]. The phase-discontinuity variable in (3.1) is suppressed to simplify notation. The barrier $V_B(x)$ is a delta-function located at the $x = 0$ plane and of strength parameter v_B (dimensionality E $_*\ell$, where E denotes the energy dimension),

$$V_B(x) = v_B\delta(x). \tag{3.2}$$

The barrier transparency is determined by the barrier's strength parameter v_B, i.e., a 'large' v_B value corresponds to weak transparency and vice-versa for 'small' v_B value. Motivated by the expressions in appendix A and previous work these limits are quantified according to the dimensionless barrier-strength parameter Z

$$v_B = \frac{Z\ k_F\hbar^2}{M} = 2\sqrt{\frac{\mu}{L}}Z, \quad L = \frac{2\ M}{\hbar^{\ 2}}, \tag{3.3}$$

where μ, M denote the chemical potential and the band-structure carrier's mass, respectively [e.g., [25, 42]. Correspondingly, $Z \gg 1$ corresponds to the weak barrier transparency while $Z \ll 1 \approx 0$ corresponds to the strong barrier transparency limits.

The two inputs to equation (3.1) are $G_0(x,\ x';\ \omega_n)$ and $\Delta(x)$ to which we turn now. For a clean metal and the delta-function barrier (3.2), the explicit expression of the Green's function is [43]

$$\begin{aligned} G_0(x,\ x';\ \omega_n) &= \left(\tfrac{i\ M}{\hbar\ \lambda}\right)e^{-i\lambda|x-x'|} + \left(\tfrac{v_B}{\hbar}\right)\left(\tfrac{i\ M}{\hbar\ \lambda}\right)^2\left(1 - \left(\tfrac{i\ M}{\hbar\ \lambda}\right)\left(\tfrac{v_B}{\hbar}\right)\right)^{-1} e^{-i\lambda(|x|+|x'|)}, \\ \lambda &= -sign(\omega_n)\sqrt{L(\mu + i\hbar\omega_n)}, \\ G_0(x,\ x';\ -\omega_n) &= \ G_0(x,\ x';\ \omega_n)|_{\lambda->\ \bar\lambda} \quad \bar\lambda = \lambda|_{\omega_n->-\omega_n}, \end{aligned} \tag{3.4}$$

For the sake of conciseness, the ω_n dependencies of λ, $\bar\lambda$ in equation (3.4) have been suppressed. The arbitrary square-root sign of λ, $\bar\lambda$ has been chosen to guarantee a negative imaginary part for all ω_n frequencies.

The other input to equation (3.1) is the energy gap $\Delta(x)$. In view of the approximation (2.5) we adopt the form

$$\Delta_{JJ}(\vec{x},\ \ \vec{x}') = \delta(\vec{x} - \vec{x}')\Delta(x)\Delta(x) = \theta(-x)\Delta_L + \theta(x)\Delta_R\ \ e^{i\psi} \tag{3.5}$$

where $\theta(x)$ denotes Heaviside step-function, ψ is the phase-discontinuity across the barrier, and Δ_L, Δ_R are the energy-gap amplitudes on the left and right sides of the barrier, respectively. While the approach below applies for arbitrary Δ_L, Δ_R values (appendix A) here we restrict ourselves to the particularly interesting cases when

$$\Delta_L = \eta\ \ \Delta_R\begin{cases}\eta = -1 & (\pi\ -\ \text{junction}) \\ \eta = 1 & (\textit{symmetric junction}).\end{cases} \tag{3.6}$$

The $\eta = -1$ case in (3.6) corresponds to two misalignment angles such that a positive energy gap on one JJ bank is aligned opposite to an equal and negative energy gap on the other bank. Such π junctions have been

demonstrated in for YBCO, with a d-wave nodal energy-gap [44]. Thus at the $x = 0$ plane there are three discontinuities: That of the delta-function barrier, the phase ψ and the energy-gap amplitude.

Solving Gorkov's equation (3.1) in real space is difficult [37, 38]. However, in momentum space an exact-solution of $G(k,\ q;\ \ \omega_n\ ;\ \psi)$ is possible, see appendix A. Recalling the definition of the double Fourier-transform of a function $\mathcal{I}\ (x,\ \ x')$ [35]

$$\mathcal{I}\ (k,\ \ q) = \int_{-\infty}^{\infty}\int_{-\infty}^{\infty} d\ x\ d\ x'\ e^{-i(k\ x - q\ x')}\mathcal{I}\ (x,\ x')\ , \tag{3.7}$$

it follows from (3.1) that the CPR is given by

$$j(x = 0;\ \psi) = \left(\frac{q_S}{4\pi^2\beta\ M}\right)\sum_{n=-\infty}^{\infty}\int_{-\infty}^{\infty}\int_{-\infty}^{\infty} dk\ dq\ \ (k + q)G(k,\ q;\ \ \omega_n\ ;\ \psi). \tag{3.8}$$

In equation (3.8) the current density is identified with its value at the barrier's location, $x = 0$. In principle the current density is location independent provided self-consistent energy gaps are employed [32, 38]. However, when a phenomenological energy gap is employed, as is commonly the case, the charge-current density continuity equation has a source-term that involves the product $\Delta(x)\ \Delta^*(x)$. To avoid this term and yet satisfy the continuity equation the current density should be evaluated at a point where $\Delta(x) = 0$, i.e. at the barrier's location $x = 0$.

Following appendix A and equation (3.6), the explicit expression for $G(k,\ \ q;\ \ \eta)$ is (dimensionality t $_*\ell$ where t denotes time)

$$\begin{aligned} G(k,\ q;\ \eta) = &\left(\frac{(k^2 - \bar{\lambda}^2)}{(k^2 - \lambda^2)(k^2 - \bar{\lambda}^2) + (L\ \ \Delta_0(\alpha))^2}\right)\times\left\{-A\delta(k - q) + \frac{F(v_B)}{q^2 - \lambda^2}\right.\\ &- \left(\frac{\Delta_0(\alpha)}{2\ \pi\hbar}\right)^2 J\ \ S(q) - \left(\left(\frac{D}{2\pi}\right)\left(\left(\frac{\eta(e^{-i\psi} - 1) + (\eta - 1)}{(k - \bar{\lambda})}\right)\right.\right.\\ &\times\left.\left(\lambda(\lambda + \bar{\lambda}) - (k + \lambda)\left(\frac{iMv_B}{\hbar^2}\right)\right)\right) - \left(\frac{\Delta_0(\alpha)}{2\ \pi\hbar}\right)^2\left(\frac{1}{2\ \bar{\lambda}}\right)H(k^2)\Bigg)P(q)\\ &- \left(\left(\frac{D}{2\pi}\right)\left(\left(\frac{\eta(e^{i\psi} - 1) + (\eta - 1)}{(k + \bar{\lambda})}\right)\left(\lambda(\lambda + \bar{\lambda}) + (k - \lambda)\left(\frac{iMv_B}{\hbar^2}\right)\right)\right)\right.\\ &+\left.\left.\left(\frac{\Delta_0(\alpha)}{2\ \pi\hbar}\right)^2\left(\frac{1}{2\ \bar{\lambda}}\right)H(k^2)\right)Q(q)\right\}. \end{aligned} \tag{3.9}$$

The known quantities $A,\ F,\ J,\ H,\ D$ in (3.9) are defined in equations (A.6), (A.7). The unknowns in equation (3.9), are defined by

$$(S(q;\ \eta),\ P(q;\ \eta),\ Q(q;\ \eta)) = \left(\int_{-\infty}^{\infty} d\ k_1\left\{\frac{1}{(k_1^2 - \lambda^2)(k_1^2 - \bar{\lambda}^2)},\ \ \frac{1}{k_1 - \bar{\lambda}},\ \ \frac{1}{k_1 + \bar{\lambda}}\right\}\times G(k_1,\ \ q;\ \ \eta)\right). \tag{3.10}$$

with self-evident notation. Since all factors in equation (3.9) are separable in the $k,\ q$ variables, the unknowns $S(q),\ P(q),\ Q(q)$ are the solutions of three coupled *linear* equations. Explicitly,

$$\begin{aligned} &\vec{V} = \vec{b} + \vec{\vec{R}}\cdot\vec{V},\quad \vec{V} = (S(q),\ P(q),\ Q(q))\\ &\vec{b} = \left(\int_{-\infty}^{\infty} d\ k_1\left\{\frac{1}{(k_1{}^2 - \lambda^2)(k_1{}^2 - \bar{\lambda}^2)},\ \frac{1}{k_1 - \bar{\lambda}},\ \frac{1}{k_1 + \bar{\lambda}}\right\}\right.\\ &\left.\times\left(\frac{G_0(k_1,\ q)(k_1{}^2 - \lambda^2)(k_1{}^2 - \bar{\lambda}^2)}{(k_1{}^2 - \lambda^2)(k_1{}^2 - \bar{\lambda}^2) + L^2\Delta_0^2(\alpha)}\right)\right), \end{aligned} \tag{3.11}$$

where the 3X3 matrix $\vec{\vec{R}}$ is obtained by employing equations (3.9), (3.10) in a straightforward way. All elements of $\vec{\vec{R}}$ (not quoted) are elementary closed-form integrals. Consequently, solving (3.11) with (3.9) yields the exact, explicit JJ Green's function expression $G(k,\ \ q;\ \ \eta)$ for an arbitrary barrier strength Z. The Green's function, equation (3.9), is a central result of this work. The corresponding CPR is given by equation (3.8) . Here we consider the CPR in the common limits when $Z \gg 1$ and $Z \ll 1 \approx 0$, corresponding to short SIS and SNS junctions respectively,

Details of the CPR calculation are deferred to appendix A. The final expression turns out simple, see below, since most terms in (3.8) drop out due to one of the following three reasons: 1. All terms involving odd $k,\ q$ powers drop in the $k,\ q$ integration. 2. When transforming the integration in the remaining terms to relative-energies variables $\xi(k) = k^2/L - \mu, \xi(q) = q^2/L - \mu$, all odd terms in $\xi(k),\quad \xi(q)$ drop in the ξ- integration.

3. All terms odd in the Matzubara frequency ω_n drop upon the frequency summation. As expected, the only surviving terms involve the phase discontinuity ψ.

Consider first the weak barrier-transparency limit when $Z \gg 1$. As shown in appendix A, in this limit, to the lowest order in $\Delta_0/\mu \ll 1$ and $1/Z$ parameters it follows that $\vec{R} \approx 0$ and $\vec{V} \approx \vec{b}$ (equation (3.11). The ensuing calculation yields the result:

$$j(x=0) = \eta \frac{q_S}{8\,Z^2\,\hbar}|\Delta_0(\alpha)|\sin(\psi)\tan h\left(\frac{\beta\ |\Delta_0(\alpha)|}{2}\right), \quad \text{for } Z \gg 1, \tag{3.12}$$

where η and $\Delta_0(\alpha)$ are defined in equations (3.6) and (1.1), respectively. The temperature dependence of $\Delta_0(\alpha)$ is suppressed to keep notation concise. The CPR (3.12) is the text-book Ambegaokar-Baratoff result with the added bonus of an explicit expression for the critical current in terms of the barrier's strength [45]. Note from (3.12) that for $\eta = -1$, i.e. for π junctions, the current flows in the 'wrong' direction [46].

In the opposite limit, when $Z \to 0$, i.e., the case of strong barrier transparency as in a SNS junctions with a thin, clean, metallic barrier the calculation is quite different. In this limit we consider only the $\eta = 1$ case. As shown in equation (A.10) and thereafter, only two diagonal $\vec{\vec{R}}$ matrix-elements equation (3.11) contribute. Employing their estimated values, equations (A.10), (A.12), in (3.11) yields for the CPR

$$\begin{aligned} j(x=0) &= \frac{q_S}{4\beta\,\hbar}\sum_{n=-\infty}^{\infty}\frac{\sin(\psi)}{|\Delta_0^2(\alpha)| + (\hbar\omega_n)^2 + \Delta_0^2(\alpha)\sin^2\left(\frac{\psi}{2}\right)\left(-\frac{\Gamma}{|\hbar\omega_n|} + \frac{1}{4}\left(\frac{\Gamma}{|\hbar\omega_n|}\right)^2\right)} \\ &\approx \frac{q_S}{4\beta\,\hbar}\sum_{n=-\infty}^{\infty}\frac{\sin(\psi)}{(\hbar\omega_n)^2 + \Delta_0^2(\alpha)\cos^2\left(\frac{\psi}{2}\right)}, \end{aligned} \tag{3.13}$$

where $\Gamma = \sqrt{\Delta_0^2(\alpha) + (\hbar\omega\ _n)^2}$. Based on the approximation $|\hbar\omega_n| \approx \langle|\hbar\omega_n|\rangle \approx |\Delta_0(\alpha)|$ we adopt $\Gamma/|\hbar\omega_n| \approx \sqrt{2}$, and the Matsubara-frequencies summation in (3.13) yields

$$j(x=0) = \left(\frac{q_S|\Delta_0(\alpha)|}{4\hbar}\right)\sin\left(\frac{\psi}{2}\right)\tan h\left(\frac{\beta|\Delta_0(\alpha)|\cos\left(\frac{\psi}{2}\right)}{2}\right), \quad \text{for } Z=0,\ \eta=1. \tag{3.14}$$

The CPR (3.14) is identical with that derived in previous work [30]. The fact that the exact Green's function (3.9) yield the correct results in the two common barrier-strength limits lends support to its veracity.

4. Discussion

4.1. Generalization to include intra-band coupling

The Green's function derived above pertains to a JJ with single energy gap superconductors. This is justified for MgB_2 in the presence of non-magnetic impurities since the two energy gaps have distinct underlying band structure [12]. In instances where that coupling cannot be ignored the approach based on the Gorkov equation (3.1) requires generalization. Details are deferred to the appendix B. Labelling the two energy gaps by 1 and 2, this generalization takes the form of two integral equations, formally written as:

$$\begin{aligned} G(\sigma \pm 1/2) = G_0(\sigma \pm 1/2) - \tfrac{1}{\hbar^2}((G_0(\sigma \pm 1/2) \bullet \Delta(\sigma \pm 1/2) \bullet \bar{G}_0(\sigma \pm 1/2) \\ \bullet\Delta^*(\sigma \pm 1/2) - |\mathcal{J}|^2 G_0(\sigma \mp 1/2) \bullet G_0(\sigma \pm 1/2))(\bullet G(\sigma \pm 1/2)),\ \ \sigma = 3/2. \end{aligned} \tag{4.1}$$

where the dot symbol $\bullet$ stands for integration on intermediate coordinates and $|\mathcal{J}|^2$ is the coupling parameter. When $|\mathcal{J}|^2 = 0$ the set equation (4.1) are two uncoupled Gorkov equations, of the type equation (3.1). For 'small' $|\mathcal{J}|^2$, as is the case in MgB_2, the correction terms in equation (4.1) can be approximated by using the uncoupled-system solutions.

4.2. Proposed experiments

Whereas in our view the data supporting an i-wave symmetry for the π energy gap is convincing, this may be the place to suggest further experiments to test this symmetry [13]. Based on experience gained with the exploration of the energy-gap symmetry in HTS, the suggestions are: 1. to make a corner SQUID made of a single MgB_2 crystal and measure the current variation as function of the magnetic flux through the SQUID's loop and 2. to make a π- JJ with crystallographically properly aligned banks and measure the spontaneous current in a loop that contains one such JJ [46–49]. The corner-SQUID approach requires a single crystal sufficiently large and

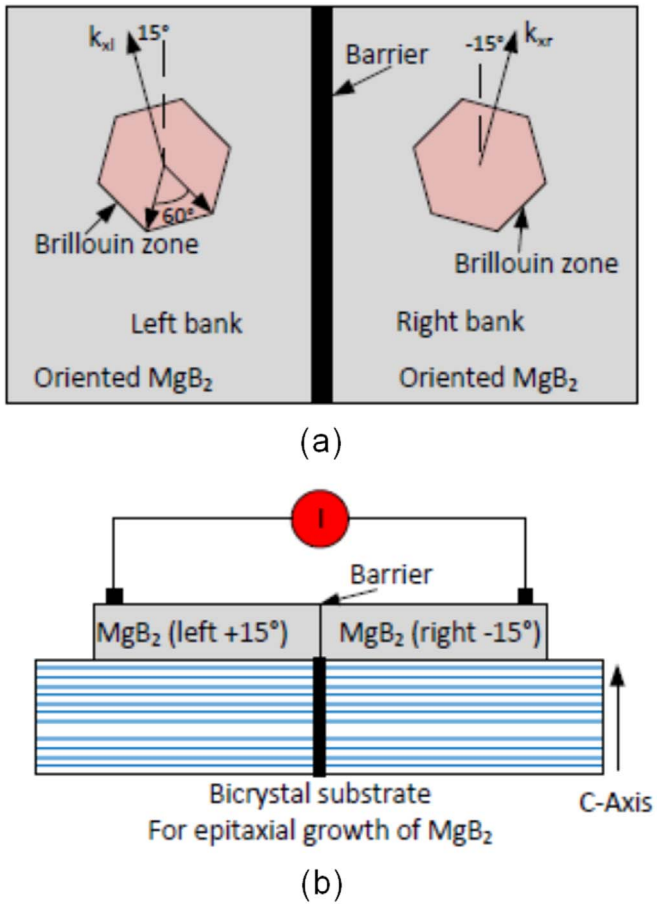

Figure 2. Schematic diagram of MgB_2 bicrystal π junction. As indicated, both JJ banks are misaligned by $|15°|$ off the crystal's x axis. (a) Top view. (b) Side view.

thick to allow attachment of two electrodes on points on its $\widetilde{ab}$ facets where the energy gap is either positive or negative. The presumed i-wave energy-gap symmetry, equation (1.1), implies energy-gap maxima at misalignment angles $15°,\ 75°,\ 135°$,... off the principal crystal $\hat{x}$ -axis, and corresponding energy-gap minima at $-15°,\ -75°,\ -135°$... The spread of either maxima or minima is $30°$, hence the precision tolerance on the electrodes' attachment-points seems achievable. A schematic π- JJ is depicted in figure 2. In analogy to the tri-crystal experiments with YBCO, the two JJ banks are single crystals where the two banks are aligned such that an energy-gap maximum on one bank faces an energy-gap minimum on the other bank [44, 50]. This experiment requires adequately aligned substrates on which to grow epitaxial MgB_2.

4.3. Summary

The simplicity of the present JJ model, i.e., the assumption of one-dimensional conduction and a delta-function barrier, comes at a price. The one-dimensional conduction ignores the angular-spread of tunneling carriers around the normal to the barrier plane. Denoting that angular-spread by $(\delta\ \theta)$, an ad-hoc way to account for this off-normal tunneling is to multiply the one-dimensional current-density expression by the factor $k_F{}^2(\delta\ \theta)/(2\ \pi)$ since only the forward Fermi-sphere hemisphere contributes [51]. Regarding the assumed delta-function barrier, this assumption excludes processes within the barrier such as dissipation, multiple Andreev reflections and magnetic-field effects such as vortex motion [11, 52, 53].

In summary, in the context of a JJ and under the approximation of one-dimensional current conduction normal to the barrier's plane, we show that a nodal energy gap with an i-wave symmetry is equivalent to an isotropic energy gap with an amplitude modified according to the misalignment angle with respect to the crystal's axes. This result and mathematical convenience suggest a focus on a JJ model with a delta function barrier of arbitrary strength. In this respect, the present work generalizes the BTK model, commonly employed for the analysis of SN tunnel junctions [25]. An explicit expression for the exact JJ Green's function is derived. The ensuing CPR is calculated in the two common limits of weak and strong barrier-strengths where we recover known CPRs, e.g., the Ambegaokar-Baratoff relation, in the strong barrier-strength limit, with an explicit

expression for the critical current in terms of the barrier's strength. While this work presupposes a single energy gap, as suggested by weak coupling between the energy gaps induced by non-magnetic defects, we outline an approach to account for such weak coupling. Following HTS experiments that established its energy-gap symmetry, we propose corresponding experiments with MgB_2 single crystals.

The authors acknowledge the support of the US Office of Naval Research and the Carderock Division of the Naval Surface Warfare Center's In-house Laboratory Independent Research Program sponsored by the Office of Naval Research administered under Program Element 0601152N.

Appendix A

Solution of Gorkov's equation (3.1)

To evaluate the complicated kernel $K(x,\ x_1;\ \omega_n;\ \psi)$, equation (3.1), it is first decomposed into spatial sectors by writing it in the form

$$K(x,\ x_1;\ \omega_n;\ \psi) = (\theta(-x) + \theta(x))\ K(x,\ x_1;\ \omega_n;\ \psi)(\theta(-x_1) + \theta(x_1)). \tag{A.1}$$

After inserting the energy gap (3.5) in equation (3.1) it breaks into the sum of eight components, compactly denoted by $K^{\pm}_{(>,<),(>,<)}$. In this notation the subscripts $(<,>)$ signify the signs of the external coordinates $(x,\ x_1)$, and the superscripts $(\pm)$ determines the sign of the intermediate integration variable x'_1.

In terms of the $K^{\pm}_{(>,<),(>,<)}$ components and after rearrangement $K(x,\ x_1;\ \omega_n;\ \psi)$ breaks into the sum of a kernel pertaining to the underlying superconductor, $K_{S\,C}$, and a term pertaining to the JJ, $K_{J\,J}$, that includes the phase discontinuity.

Explicitly

$$K(x,\ x_1;\ \omega;\ \psi;\ \eta) = K_{S\,C}(\eta;\ \psi = 0) + K_{JJ}(\eta;\ \psi), \tag{A.2}$$

where

$$\begin{aligned}
&K_{S\,C}(\eta;\ \psi = 0) = \Delta_0^2(\alpha)\tilde{K}^{(ALL)} + (\eta - 1)(K^{(-)}_{<,>} + K^{(-)}_{>,>} + K^{(+)}_{>,<} + K^{(+)}_{<,<}) \\
&\tilde{K}^{(ALL)} = \left(\tfrac{1}{\hbar}\right)^2 \int_{-\infty}^{\infty} dy_1 G_0(x,\ y_1;\ \omega_n) G_0(x_1,\ y_1;\ -\omega_n) \\
&K_{JJ}(\eta;\ \psi) = \eta((e^{-i\psi} - 1)(K^{(-)}_{<,>} + K^{(-)}_{>,>}) + (e^{i\psi} - 1)(K^{(+)}_{>,<} + K^{(+)}_{<,<})), \quad \eta = \pm 1
\end{aligned} \tag{A.3}$$

where

$$\begin{aligned}
K^{(+)}_{<,<} &= \theta(-x)\theta(-x_1)\left(\frac{\Delta_0(\alpha)}{\hbar}\right)^2 \int_0^{\infty} d\ y_1\ G_0(x,\ y_1;\ \omega_n) G_0(x_1,\ y_1;\ -\omega_n) = \Delta_0^2(\alpha)\tilde{K}^{(+)}_{<,<} \\
K^{(-)}_{<,>} &= \theta(-x)\theta(x_1)\left(\frac{\Delta_0(\alpha)}{\hbar}\right)^2 \int_{-\infty}^{0} d\ y_1 G_0(x,\ y_1;\ \omega_n) G_0(x_1,\ y_1;\ -\omega_n) = \Delta_0^2(\alpha)\tilde{K}^{(-)}_{<,>} \\
K^{(+)}_{>,<} &= \theta(x)\theta(-x_1)\left(\frac{\Delta_0(\alpha)}{\hbar}\right)^2 \int_0^{\infty} d\ y_1 G_0(x,\ y_1;\ \omega_n) G_0(x_1,\ y_1;\ -\omega_n) = \Delta_0^2(\alpha)\tilde{K}^{(+)}_{>,<} \\
K^{(-)}_{>,>} &= \theta(x)\theta(x_1)\left(\frac{\Delta_0(\alpha)}{\hbar}\right)^2 \int_{-\infty}^{0} d\ y_1 G_0(x,\ y_1;\ \omega_n) G_0(x_1,\ y_1;\ -\omega_n) = \Delta_0^2(\alpha)\tilde{K}^{(-)}_{>,>}
\end{aligned} \tag{A.4}$$

Decomposition (A.2) guarantees that in the absence of the phase-discontinuity ψ the underlying superconductor kernel is automatically recovered.

In momentum space, equation (3.7), the Gorkov's equation (3.1) takes the form

$$G(k,\ q) = G_0(k,\ q) - \left(\frac{1}{2\pi}\right) \int_{-\infty}^{\infty} d\ q_1\ K(k,\ q_1)\ G(q_1,\ q) \tag{A.5}$$

where dependencies on some variables in have been suppressed to simplify notation. Employing (3.4), the integrations in (A.2) yield the following explicit expressions:

$$G_0(k,\,q) = \left(\frac{1}{k^2-\lambda^2}\right)\left(-A\delta(k-q) + \frac{F(\nu_B)}{q^2-\lambda^2}\right),$$
$$A = \left(\frac{4\,\pi\,M}{\hbar}\right), \quad F(\nu_B) = \frac{4\,i\,M^2\lambda\;\nu_{\mathbf{B}}}{\hbar(M\,\nu_B + i\,\lambda\,\hbar^2)}, \quad \bar{F}(\nu_B) = F(\nu_B)|_{\lambda\,\rightarrow\,\bar{\lambda}}$$
$$K_{\,SC}(k,\;q;\,\eta=1) = \frac{\Delta_0^2(\alpha)}{2\,\pi\,\hbar^2(k^2-\lambda^2)}\left(A^{\,2}\frac{\delta(k-q)}{q^2-\bar{\lambda}^2} + \frac{H(k^2)}{2\bar{\lambda}}\left(\frac{1}{q-\bar{\lambda}} - \frac{1}{q+\bar{\lambda}}\right) + \frac{J}{(q^2-\lambda^2)(q^2-\bar{\lambda}^2)}\right)$$
$$H(k^2) = -A\frac{\bar{F}(\nu_B)}{k^2-\bar{\lambda}^2} + \frac{i\,\pi F(\nu_B)\bar{F}(\nu_B)}{\lambda\,\bar{\lambda}(\lambda+\bar{\lambda})}, \quad J = -AF(\nu_B) \tag{A.6}$$

and

$$\begin{Bmatrix} K^{(-)}_{>,\,>} + & K^{(-)}_{<,\,>} \\ K^{(+)}_{<,\,<} + & K^{(+)}_{>,\,<} \end{Bmatrix}(k,\,q) = \left(\frac{D}{k^2-\lambda^2}\right)\begin{Bmatrix} \frac{1}{(k-\bar{\lambda})(q-\bar{\lambda})}\left(\lambda(\lambda+\bar{\lambda}) - (k+\lambda)\left(\frac{i\,M\,\nu_B}{\hbar^2}\right)\right) \\ \frac{1}{(k+\bar{\lambda})(q+\bar{\lambda})}\left(\lambda(\lambda+\bar{\lambda}) + (k-\lambda)\left(\frac{i\,M\,\nu_B}{\hbar^2}\right)\right) \end{Bmatrix}$$
$$D(\nu_B) = \Delta_0^2(\alpha)\,\frac{i\,\hbar^2F(\nu_B)\bar{F}(\nu_B)}{6\,\lambda\,\bar{\lambda}\,(\lambda+\bar{\lambda})M^2\nu_B^{\,2}} \tag{A.7}$$

A key advantage of the above Fourier transformation is that all components in equations (A.6), (A.7) are separable in the k, q variables. This property allows for the solution of the unknowns (3.10) in closed form, see equation (3.9).

In the 'Born' approximation we take $\vec{V} = \vec{b}$ and $G(k,\,q)|_{\,BORN} = G_0(k,\,q)$, equation (3.11). At low temperatures, when $\beta|\Delta_0(\alpha)| \gg 1$, the estimated ratio between the two terms in $G_0(k,\,q)$, equation (A.6), implies that the delta-function term dominates for low and high Z values. Correspondingly, the Born approximation (3.11) in this temperature regime is

$$\vec{b} = -\frac{A}{(q^2-\lambda^2)(q^2-\bar{\lambda}^2) + L^2\Delta_0^2}\left(\frac{1}{q^2-\lambda^2},\;\; q+\bar{\lambda},\;\; q-\bar{\lambda}\right) \tag{A.8}$$

Next we evaluate the matrix $\vec{\vec{R}}$ in equation (3.11). Consider first the weak transparency regime, $Z \rightarrow \infty$. In that limit $F(Z\rightarrow\infty) \approx 4\,i\,M\lambda/\hbar$, $\bar{F}(Z\rightarrow\infty) \approx 4\,i\,M\bar{\lambda}/\hbar$ and provided $\mu \gg \Delta_{\,0} \approx \langle|\hbar\omega_{\,n}|\rangle$, it follows that

$$H(k^2) \propto \frac{\bar{\lambda}}{k^2-\bar{\lambda}^2} + \frac{1}{\lambda+\bar{\lambda}} \approx \frac{1}{i\,|\hbar\omega|}\sqrt{\frac{\mu}{L}} + \frac{1}{-i\,|\hbar\omega|}\sqrt{\frac{\mu}{L}} = 0. \tag{A.9}$$

Consequently, for the matrix $\vec{\vec{R}}$, equation (3.11),
$R_{P,P} = -R_{P,Q} = -R_{Q,Q} = R_{Q,P} = 0$, $\quad R_{S,P} = -R_{S,Q} = 0$. Likewise in the opposite limit, when $\beta\,|\Delta_0(\alpha)| \gg 1$, estimates of the remaining matrix elements $R_{P,S} = -R_{Q,S}$ implies that they can be neglected as well. All in all it follows that for $\vec{\vec{R}}(Z\rightarrow\infty) \approx 0$ and the Born expressions for $\vec{V} = (S(q),\,P(q),\,Q(q))$ provide an excellent approximation. The corresponding CPR is the Ambegaokar-Baratoff result.

Consider now the opposite limit, when $Z \rightarrow 0$, e.g., SNS junctions with a thin N barrier. We consider only the $\eta = 1$ case. In this limit, the Born approximation, eqaution (A.8), remains unchanged. However, the unknown $S(q)$ drops out since to lowest order in Z we have $F(\nu_B) = 0$ and the matrix $\vec{\vec{R}}$, equation (3.11), $R_{S,P} = R_{S,Q} = R_{P,S} = R_{Q,S} = 0$. The terms that contribute to the matrix $\vec{\vec{R}}$ are those that involve the phase ψ. Explicitly,

$$R_{P,P} = (e^{-i\,\psi} - 1)I_D, \quad R_{Q,Q} = (e^{+\,i\,\psi} - 1)I_D,$$
$$R_{P,Q} = (e^{+\,i\,\psi} - 1)I_{ND}, \quad R_{Q,P} = (e^{-\,i\,\psi} - 1)I_{ND}. \tag{A.10}$$

Furthermore, simple estimate yields that $|I_{ND}|/|I_D| \approx |\Delta_{\,0}|/\mu \ll 1$. Hence the only contribution to $\vec{\vec{R}}$ are the two diagonal elements proportional to the dimensionless integral I_D. This quantity is estimated as follows

$$I_D \propto \int d\,\bar{k}\left(\frac{\bar{k}+\bar{\lambda}}{\bar{k}-\bar{\lambda}}\right)\frac{1}{(\bar{k}^2-\lambda^2)(\bar{k}^2-\bar{\lambda}^2) + L^2\,|\,\Delta_0^2\,|} = \frac{1}{2L^2}\sqrt{\frac{L}{\mu}}\int d\,\xi$$
$$\times\,\frac{\xi + 2\mu - i\,\hbar\omega}{(\xi + i\,\hbar\omega)(\xi^2 + (\hbar\omega)^2 + |\,\Delta_0^2\,|)} \approx \frac{\pi\,\mu}{i\,\hbar\omega\,\Gamma}\sqrt{\frac{L}{\mu}}, \;\; \Gamma = \sqrt{(\hbar\omega)^2 + |\Delta_0^2|}, \tag{A.11}$$

where the relations $k^2 = L(\xi+\mu)$, $\quad \bar{\lambda}^2 = L(\mu - i\,\hbar\omega) \approx L\mu$, $\quad \lambda^2 = L(\mu + i\,\hbar\omega)$ have been employed. This yields for I_D the estimate

$$I_D = -\frac{|\Delta_0^2|}{4|\hbar\omega_n|\ \Gamma} \quad (\eta = 1), \tag{A.12}$$

which leads to the CPR equation (3.14).

In this part of the appendix we *outline* generalization of the above approach to the general case where. Equation (3.5) holds yet not equation (3.6). Define the following additional (divergent) quantities

$$\tilde{K}^{(-)}_{<,<} = \theta(-x)\theta(-x_1)\left(\frac{1}{\hbar}\right)^2 \int_{-\infty}^{0} d\ y_1\ G_0(x,\ y_1;\ \omega_n) G_0(x_1,\ y_1;\ -\omega_n)$$
$$\tilde{K}^{(+)}_{>,>} = \theta(x)\theta(x_1)\left(\frac{1}{\hbar}\right)^2 \int_{0}^{\infty} d\ y_1\ G_0(x,\ y_1;\ \omega_n) G_0(x_1,\ y_1;\ -\omega_n). \tag{A.13}$$

In terms of the quantities (A.13) the kernel $K(x,\ x_1)$ of equation (3.1) breaks down as follows:

$$K_{SC} = \Delta_L^2 \tilde{K}^{(-)}_{<,<} + \Delta_{\ L}\Delta_{\ R}\tilde{K}^{(+)}_{<,<} + \Delta^2{}_L \tilde{K}^{(-)}_{>,<} + \Delta_L\Delta_{\ R}\tilde{K}^{(+)}_{>,<}$$
$$+ \Delta^2{}_R \tilde{K}^{(+)}_{<,>} + \Delta_L\Delta_R\tilde{K}^{(-)}_{<,>} + \Delta^2{}_R\tilde{K}^{(+)}_{>,>} + \Delta_L\Delta_R\tilde{K}^{(-)}_{>,>}$$
$$K_{JJ} = \Delta_L\Delta_R((e^{-\ i\ \psi} - 1)(\tilde{K}^{(-)}_{<,>} + \tilde{K}^{(-)}_{>,>}) + (e^{i\psi} - 1)(\tilde{K}^{(+)}_{>,<} + \tilde{K}^{(+)}_{<,<})), \tag{A.14}$$

As the K_{JJ} term in equation (A.14) indicates, the CPR is proportional to the product to $\Delta_L\Delta_R$, consistent with previous results based on group-theoretic considerations [29]. After some rearrangement the kernel K_{SC} can be rewritten as follows

$$K_{S\,C} = \langle\Delta^2\rangle\tilde{K}^{(ALL)} + (\delta\ \Delta^2)((\tilde{K}^{(-)}_{<,<} + \tilde{K}^{(+)}_{<,<}) - (\tilde{K}^{(+)}_{>,>} + \tilde{K}^{(-)}_{>,>}) + (\tilde{K}^{(-)}_{>,<} + \tilde{K}^{(+)}_{>,<}) - (\tilde{K}^{(+)}_{<,>} + \tilde{K}^{(-)}_{<,>}))$$
$$+ (\Delta_R - \Delta_L)(\Delta_L(\tilde{K}^{(+)}_{<,<} + \tilde{K}^{(+)}_{>,<}) - \Delta_R(\tilde{K}^{(-)}_{<,>} + \tilde{K}^{(-)}_{>,>})),\quad \langle\Delta^2\rangle = \frac{\Delta_L^2 + \Delta_R^2}{2},$$
$$(\delta\Delta^2) = \frac{\Delta_L^2 - \Delta_R^2}{2}. \tag{A.15}$$

The first term in the RHS of (A.15) has an analytical Fourier transform, equation (A.6). Consider now the particular energy-gap relation, equation (3.6). When $\eta = 1$, which is the symmetrical JJ, the second and third terms on the RHS of (A.15) vanish. When $\eta = -1$, which is a symmetrical $\pi-$ JJ, the term proportional to $(\delta\ \Delta^2)$ vanishes while the third term on the RHS of (A.15) is proportional to $-2\ \Delta^2{}_L = -2\ \Delta^2{}_R$, as in equation (3.9). In the corresponding $Z \to \infty$, the structure of the CPR, equation (3.12) remains unchanged. When the energy gaps of both banks are not related as in equation (3.6), e.g., in a JJ where one bank is nodal while the other is a proper s-wave superconductor the above-generalized approach should be applied [47].

Appendix B

Gorkov's equation for two coupled energy bands

Consider two energy bands labelled by 1 and 2. The corresponding 4×4 matrix Gorkov's equation takes then the formal form

$$\ddot{\mathbb{Q}} \cdot \hat{G} = \hbar\delta(x - x')\ddot{1},\quad \hat{G} = -\langle T_{\ \tau}[\hat{\Psi}(\vec{x},\ \tau)\hat{\Psi}^{\dagger}(\vec{x},\ \tau)]\rangle. \tag{B.1}$$

In (B.1) the symbol $\hat{G}$ denotes the 4X4 Green function matrix, $x = (\vec{x},\ \ \tau)$ where $\tau = it$ denotes the imaginary time, and $T_{\ \tau}$ is the time-ordering operator [35].

For the case where the two energy bands are coupled by a parameter $\mathcal{I}$, the symbols in (B.1) are given by

$$\hat{\Psi}(\vec{x},\ \tau) = \begin{pmatrix} \psi_1 \\ \psi^{\dagger}{}_1 \\ \psi_2 \\ \psi^{\dagger}{}_2 \end{pmatrix},\quad \ddot{\mathbb{Q}} = \begin{pmatrix} \hat{D}_{\ 1} & \Delta_1 & \mathcal{I} & 0 \\ \Delta^*{}_1 & -\hat{\bar{D}}_{\ 1} & 0 & \mathcal{I}^* \\ \mathcal{I}^* & 0 & \hat{D}_{\ 2} & \Delta_2 \\ 0 & \mathcal{I} & \Delta^*{}_2 & -\hat{\bar{D}}_{\ 2} \end{pmatrix},$$
$$\hat{D} = -\hbar\frac{\partial}{\partial\tau} - (H_B(\hat{\vec{p}}) - \mu),\quad \hat{\bar{D}} = \hbar\frac{\partial}{\partial\tau} - (H_B(\hat{\vec{p}}^*) - \mu). \tag{B.2}$$

where pairing between carriers belonging to different bands is neglected [54]. The symbol $H_B(\hat{\vec{p}})$ in equation (B.2) denotes the band-structure Hamiltonian.

At this point we use the following formal relations [35]

$$G_0 = \hbar\ \hat{D}^{-\ 1}\delta(x - x'), \quad \bar{G}_0 = \hbar\ \hat{\bar{D}}^{-\ 1}\delta(x - x'),$$
$$F_i = -\langle T_\tau[\psi_i(\vec{x}, \tau)\psi_i(\vec{x}', \tau')]\rangle, \quad G_{\ i,\ j} = -\langle T_\tau[\psi_i(\vec{x}, \tau)\psi_j{}^\dagger(\vec{x}', \tau')]\rangle,$$
$$\Delta_i(\vec{x} - \vec{x}') = -g\langle T_\tau[\psi_i(\vec{x}, \tau)\psi_i(\vec{x}', \tau')]\rangle, \tag{B.3}$$

Evaluation of the first and third rows in (B.1) yields equation (4.1).

ORCID iDs

Daniel E Oates https://orcid.org/0000-0003-1971-6263

References

[1] Canfield P C and Crabtree G W 2003 *Phys. Today* **56** 34
[2] Eisterer M 2007 *Supercond. Sci and Technol.* **20** R47
[3] Xi X X 2008 *Rep. Prog. Phys.* **71** 116501
[4] Bueza C and Yamashta T 2001 *Supercond. Sci and Technol.* **14** R115
[5] Zehetmayer M 2013 *Supercond. Scie. and Tech.* **26** 043001
[6] Collings E W, Sumption M D, Bhatia M, Susner M A and Bohnenstiehl S D 2008 *Supercond. Scie. and Tech.* **21** 103001
[7] Pei X, Smith A C, Husband M and Rindfleish A M 2012 *Trans. of Applied. Supercond.* **22** 5600405
[8] Withanage W, Lee N H, Penmatsa S, Wolak M A, Nassiri A and Xi X X 2017 *Phys. Rev. Accel. Beams* **20** 102002
[9] Tajima T, Civale L, Delvin D J, Schulze R K, Osov I O and Martinez G C 2013 *Proc. SRF2013, Paris, France*
[10] Guo Z, Cai X, Liao X, Chen Y, Yang C, Niu R, Luo W, Huang Z, Feng Q and Gan Z 2018 *Supercond. Sci. Technol.* **31** 065005
[11] Chen K, Zhuang C G, Li Q, Zhu Y, Voyles P M, Weng X, Redwing J M, Singh R K, Kleinsasser A W and Xi X X 2010 *App. Phys. Lett.* **96** 042506
[12] Mazin I I, Andersen O K, Jepsen O, Dolgov O V, Kortus J, Golubov A A, Kuzmenko A B and van der Marel D 2002 *Phys. Rev. Lett.* **89** 107002
[13] Agassi Y D and Oates D E 2017 *Supercond. Scie. and Technolog.* **30** 115015
[14] Agassi Y D, Oates D E and Moeckly B H 2012 *Physica C* **480** 79
[15] Agassi Y D, Oates D E and Moeckly B H 2009 *Phys. Rev. B* **80** 174522
[16] Yip S K and Sauls J A 1995 *Phys. Rev. B* **51** 16233
[17] Dahm T and Scalapino D J 1999 *Phys. Rev. B* **60** 13125
[18] Brinkman A, Golubov A A, Rogala H, Dolgov O V, Kortus J, Kong Y, Jepsen O and Andersen O K 2002 *Phys. Rev. B* **65** 180517 (R),
[19] Dolgov O V, Gonnelli R S, Ummarino G A, Golubov A A, Shulga S V and Kortus J 2003 *Phys. Rev. B* **68** 132503
[20] Dahm T 2005 *Frontiers in Superconducting Materials* ed A V Narlikar (Berlin: Springer) p. 983
[21] Mazin I I and Kortus J 2002 *Phys. Rev. B* **65** 180510
[22] Chen K, Cunnane D, Shen Y, Xi X X, Kleinsasser A W and Rowell J 2012 *App/ Phys. Lett.* **100** 122601
[23] Shen Y, Singh R K, Sanghavi S, Wei Y, Chamberlin R V, Moeckly B H, Rowell J M and Newman N 2010 *Supercond. Scie. and Technolog.* **21** 075003
[24] Costache M V and Moodera J M 2010 *App. Phys. Lett.* **96** 082508 and references therein
[25] Blonder G E, Tinkham M and Klapwijk T M 1982 *Phys. Rev. B* **25** 4515
[26] Octavio M, Tinkham M, Blonder G E and Klapwijk T M 1983 *Phys. Rev. B* **27** 6739
[27] Furusaki A 1999 *Superlattices Microstruct.* **25** 809
[28] Sigrist M and Rice T M 1992 *J. Phys. Soc. Japan* **61** 4283
[29] Tsui C C and Kirtley J R 2000 *Rev. Mod. Phys.* **72** 969
[30] Furusaki A, Takayanagi H and Tsukada M 1992 *Phys. Rev. B* **45** 10563
[31] Agassi D and Cullen J R 1996 *Phys. Rev. B* **54** 10112
[32] Bottcher K and Kopp T 1997 *Phys. Rev. B* **55** 11670
[33] Ambegaokar V and Baratoff A 1963 *Phys. Rev. Lett.* **10** 486
Ambegaokar V and Baratoff A 1963 *Phys. Rev. Lett.* **11** 104 (Errata)
[34] Abrikosov A A, Gorkov L P and Dzyaloshinski I E 1963 *Methods of Quantum Field Theory in Statistical Physics* (New York: Dover Publications, Inc.)
[35] Fetter A L and Walecka J D 1971 *Quantum Theory of Many-Particle Systems* (New York: McGraw-Hill Book Company)
[36] Flatte M E and Byers J M 1997 *Phys. Rev. B* **56** 11213 ; M E Flatte and J M Byers in 1999 'Solid State Physics', H Ehrenreich and F Spaeoen, Editors (San Diego: Academic Press) p 138
[37] Feuchtwang T E 1974 *Phys. Rev. B* **10** 4135
[38] Furusaki A and Tsukada M 1991 *Solid State Comm.* **78** 299
[39] Barone A and Paterno G 1982 *Physics and Applications of the Josephson Efect* (New York: Wiley-Interscience Publication)
[40] Arfken G B and Weber H J 2005 *Mathematical Methods for Physicists* (Amsterdam: Elsevier) p 687
[41] Fetter A L and Walecka J D 1971 *Quantum Theory of Many-Particle Systems* (New York: McGraw-Hill Book Company) p467
[42] Tanaka Y and Kashiwaya S 1995 *Phys. Rev. Lett.* **74** 3451
[43] Kulik I O and Yanson I K 1972 *The Josephson effect in superconductive tunneling structures* (Jerusalem: Israel Program for Scientific Translations)
[44] Schulz R R, Chesca B, Schneider C W, Schmehl A, Bielefelt H, Hilgenkamp H and Mannhart J 2000 *App. Phys. Lett.* **76** 912
[45] Tinkham M 1996 *Introduction to Superconductivity* (New York: McGraw-Hill, Inc) p. 200
[46] Bulaevskii L M, Kuzii V V and Sobyanin A A 1977 *JETP Lett.* **25** 290
[47] Harlingen D J V 1995 *Rev. Mod. Phys.* **67** 515

[48] Bauer A, Bentner J, Aprili A, Della Rocca M L, Reinwald M, Wegscheider W and Strunk C 2004 *Phys. Rev. Lett.* **92** 217001
[49] Alff L, Kleefisch S, Schoop U, Zittarz M, Kemen T, Bauch T, Marx A and Gross R 1998 *Eur. Phys. J. B* **5** 423
[50] Tsuei C C, Kirtley J R, Chi C C, Jahnes L Y, Gupta A, Shaw T, Sun J Z and Ketchen M B 1994 *Phys. Rev. Lett.* **73** 593
[51] Fogelstrom M, Rainer D and Sauls J A 1997 *Phys. Rev. Lett.* **79** 281
[52] Kulik I O 1970 *Sov. Phys. JETP* **30** 944
[53] Lofwander T, Shumeiko V S and Wendin G 2001 *Supercond. Sci. Technol.* **14** R53
[54] Agassi Y D and Oates D E 2014 *Physica C* **506** 119